LA-UR-01-3261
Approved for public release;
distribution is unlimited.

Title: **DIAMETER EFFECT CURVE AND DETONATION FRONT CURVATURE MEASUREMENTS FOR ANFO**

Author(s): R. A. Catanach & L. G. Hill

Submitted to:

http://lib-www.lanl.gov/cgi-bin/getfile?00796877.pdf

DIAMETER EFFECT CURVE AND DETONATION FRONT CURVATURE MEASUREMENTS FOR ANFO*

R. A. Catanach & L. G. Hill

Los Alamos National Laboratory
Los Alamos, New Mexico 87545 USA

Diameter effect and front curvature measurements are reported for rate stick experiments on commercially available prilled ANFO (ammonium-nitrate/fuel-oil) at ambient temperature. The shots were fired in paper tubes so as to provide minimal confinement. Diameters ranged from 77 mm (≈ failure diameter) to 205 mm, with the tube length being ten diameters in all cases. Each detonation wave shape was fit with an analytic form, from which the local normal velocity D_n, and local total curvature κ, were generated as a function of radius R, then plotted parametrically to generate a $D_n(\kappa)$ function. The observed behavior deviates substantially from that of previous explosives, for which curves for different diameters overlay well for small κ but diverge for large κ, and for which κ increases monotonically with R. For ANFO, we find that $D_n(\kappa)$ curves for individual sticks 1) show little or no overlap—with smaller sticks lying to the right of larger ones, 2) exhibit a large velocity deficit with little κ variation, and 3) reach a peak κ at an intermediate R.

INTRODUCTION

Rate stick tests on lightly confined prilled ANFO at ambient temperature were conducted to measure steady-state detonation velocity and detonation front curvature as a function of diameter. It is well known that ANFO's detonation velocity varies considerably with charge diameter. Yancik[1], Petes[2], and others have shown that several other physical properties can affect ANFO's detonation velocity. These include the type of confinement, explosive density, particle size and distribution, fuel oil content, moisture content and temperature. Furthermore, these factors can be interdependent. Differences in detonation velocity can also be attributed to slightly different physical properties of the ammonium nitrate (AN) produced by different manufacturers. Because there are no standard specifications by which AN is produced, batch-to-batch variation from a single production plant is not uncommon. Although performance data for ANFO have been studied for over four decades and become somewhat self-consistent since being introduced in the mid-1950's, variability in performance can still be expected from this highly non-ideal explosive.

Near critical diameter, ANFO exhibits a severe velocity deficit; however, with increasing diameter a slight upturn in the diameter effect curve is observed. We developed an extension of the widely used Campbell/Engelke[3] curve fit that accurately captures both behaviors together.

The detonation velocity of a given explosive is also related to the detonation front curvature[4], which is the basis of Detonation Shock Dynamics (DSD) theory[5]. Very little such data exists on ANFO. A study by Sandstrom[6] on an ANFO rate stick confined in polyvinyl chloride showed a jagged, saw-toothed detonation wave front. This is expected due to the large granular features of the ANFO prills. In this study we measured front curvature of several ANFO rate sticks of varying diameters in paper tube confinement, and discovered a similar wave front pattern. Each wave front was analyzed in a manner similar to those of previous PBX 9502[7] and nitromethane[8] tests. The generated $D_n(\kappa)$ curves indicate that ANFO exhibits a behavior that is significantly different from other explosives.

* Work supported by the United States Department of Energy.

EXPERIMENT

Our ANFO was composed of commercial (Titan Energy, Lot No. 30SE99C) explosive grade AN prills, with 6 wt.% diesel fuel. Separate bags were well blended prior to firing, to obtain consistent samples and to minimize batch-to-batch variability.

Twelve rate sticks were fired at ambient temperature in thin wall (6 mm) paper tubes. Seven diameters were tested between 77 and 205 mm inner diameter (ID). Three cases were successfully repeated to obtain duplicate front curvatures. The length-to-diameter (L/D) ratio was 10 in all cases. The charges were fired in a vertical position to 1) accommodate top loading, 2) record detonation front curvature at the bottom, and 3) obtain an axially symmetric density distribution to minimize wave tilt. A schematic diagram is shown in Fig. 1.

Each charge was loaded in ten separate lifts —except for the 205 mm stick, which required twenty lifts—to attain a uniform density throughout the charge. Individual lifts were weighed prior to pouring. During the pour of each lift, the outside of the tube was gently tapped. The top of each lift was lightly tamped with a flat-bottomed plunger to provide a level prill distribution between lifts. The rise height of each lift was measured and the density per lift calculated. This procedure gave a bulk density of approximately 0.90 g/cc. The shots were boosted using pressed PBX 9501 cylinders. These had the same ID as the tubes, and a L/D ratio of 1/2.

The detonation velocity was measured using eleven self-shorting capped shock pins glued into holes drilled at equal intervals along the tube. The shorting pins were inserted flush with the ID of the tube starting four diameters from the top of the rate stick. The eleven shorting pins were connected to a Los Alamos DM-11 pin board and multiplexed to a single cable so that when the detonation wave shorts the pin, it fires an RC circuit in the pin board, producing a short voltage pulse.

To measure detonation front curvature, the rate sticks were capped at the bottom with a PMMA window. A small strip of PETN paint was applied across the diameter of the inside window surface; this served as a flasher. It was applied in a thin layer and covered with copper tape to block reaction prelight from the detonation front, which scatters 20 to 30 mm ahead of the wave front.[9] Front curvature was recorded with a rotating mirror streak camera at a writing speed of 1 mm/μsec.

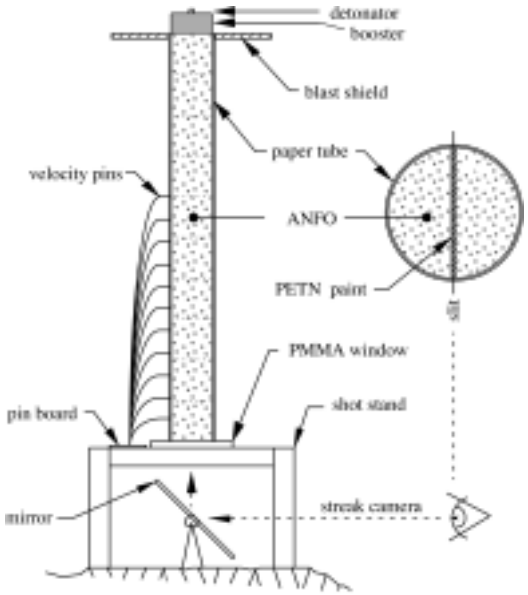

Figure 1. Schematic diagram of ANFO rate stick experiment.

ANALYSIS

A linear least squares fit was applied to the *x*-*t* pin data to obtain the axial detonation velocity, D_0, for each rate stick. Of the seven diameters tested, five were repeated to investigate velocity repeatability. For all the tests, a minimum of nine pin signals were recorded. The average standard velocity error for all the tests, excluding the test that reached failure diameter, was ± 2.7 m/s. The velocity for the test at failure diameter was recorded in the process of failing, with the first ten of eleven pins reporting.

The film records were read on an optical comparator from edge to edge. The center was then computed as the average of the left and right edges, and the two sides were partitioned. The magnifica- tion was measured from either a scale taped adjacent to the PETN strip, or a still exposure of the tube ID.

The processed film data gives breakout time *t* as a function of the radius *r*. When the two sides are overlaid the data generally do not overlay to within experimental noise. The reason is wave tilt. We applied a linear tilt correction (i.e., for the tilt component in the slit direction) based upon a linear least squares fit to the time difference, as a function of *r*, between the left and right data sets. When tilt-corrected records are overlaid, the data scatter from both sides combined is comparable to that for each side alone. Inferred tilt angles are shown in Table 1.

TABLE 1. Diameter Effect and Wave Front Data (Mean $T_0 \approx 19°C$ and Relative Humidity ≈ 30%)

Charge Diameter ∅ (mm)	Charge Density ρ (g/cc)	Detonation Velocity D_0 (mm/μs)	Fit Coefficient a_1 (mm)	Fit Coefficient η	z/R Max.	Edge Angle (degrees)	Tilt Angle (degrees)	Shot Number
77	0.91	1.68	*	*	*	*	*	3850
90	0.89	2.41	25.32	0.7126	0.4694	52.6	0.53	3849
90	0.93	2.47	—	—	—	—	—	3851
102	0.89	2.79	36.96	0.6389	0.4689	49.9	0.93	3853
102	0.88	2.82	—	—	—	—	—	3846
115	0.88	2.99	37.33	0.6522	0.4221	47.4	0.21	3847
115	0.92	3.01	40.50	0.6504	0.4573	49.6	0.26	3852
128	0.92	3.18	47.76	0.6270	0.4424	47.9	0.20	3854
128	0.92	3.22	41.64	0.6641	0.4484	49.5	0.03	3855
153	0.90	3.46	52.58	0.6425	0.4337	47.8	0.14	3857
153	0.91	3.51	54.01	0.6358	0.4314	47.5	0.18	3848
205	0.91	3.92	64.93	0.6471	0.4068	46.1	0.34	3856
5300	≈ 0.88	4.94	—	—	—	—	—	(2)
9100	≈ 0.91	5.26	—	—	—	—	—	(2)

* failed

Given that a detonation in a stick approaches a steady traveling wave after propagating a few diameters, the wave shape z as a function of r is

$$z(r) = D_0\, t(r). \qquad (1)$$

The $z(r)$ data is fit to the series

$$z(r) = -\sum_{i=1}^{n} a_i \left(\ln\left[\cos\left[\eta \frac{\pi}{2} \frac{r}{R} \right] \right] \right)^i , \qquad (2)$$

where R is the charge radius and a_i and η are fitting parameters, with $0 \le \eta \le 1$ controlling the curvature near the edge. One should not use a higher order fit than necessary, or spurious wiggles will occur. In this case (cf. 7,8), only the first term was necessary to fit wave shapes to within random scatter, as shown for Shot #3856 in Fig. 2. The granular nature of the ANFO produced some outlier points that were dropped if the standard error improved by doing so.

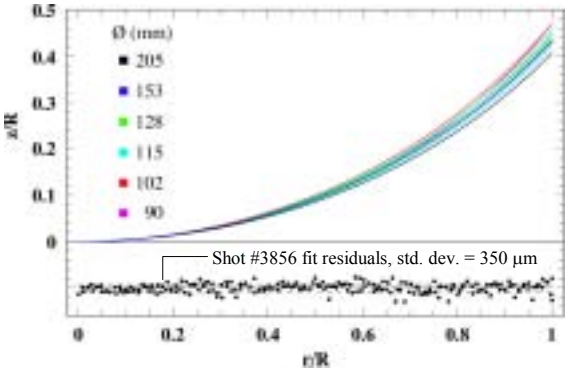

FIGURE 2. Wave shape curve fits and fit residuals (#3856).

RESULTS

Figure 2 shows that—with the exception of Shot #3847—wave profiles normalized by R are progressively flatter for larger charges than for smaller ones. This is the typical and expected behavior.

The diameter effect data are listed in Table 1. Two data points from the *Dice Throw* program of large unconfined ANFO charges that were fired at a similar density are included from Petes[2]. Diameter effect data have traditionally been fit using the form[3]

$$\frac{D_0}{D_\infty} = 1 - \frac{A}{R - R_c} , \qquad (3)$$

where D_∞ is the Chapman-Jouguet velocity, and A and R_c are fitting parameters. We prefer to express Eq. 3 in "diameter effect" coordinates as

$$\frac{D_0}{D_\infty} = 1 - \frac{\beta k}{k_d - k} , \qquad (4)$$

where $k = 1/R$, $k_d = 1/R_c$, and β is a dimensionless fitting parameter. Our extension involves replacing unity by the term $\frac{k_u - \alpha k}{k_u + k}$, so that

$$\frac{D_0}{D_\infty} = \frac{k_u - \alpha k}{k_u + k} - \frac{\beta k}{k_d - k} , \qquad (5)$$

where Eq. 4 is recovered if $\alpha \to -1$. Approximately, k_u and k_d characterize the position of the upturn and downturn, respectively, while α and β are dimensionless shape factors.

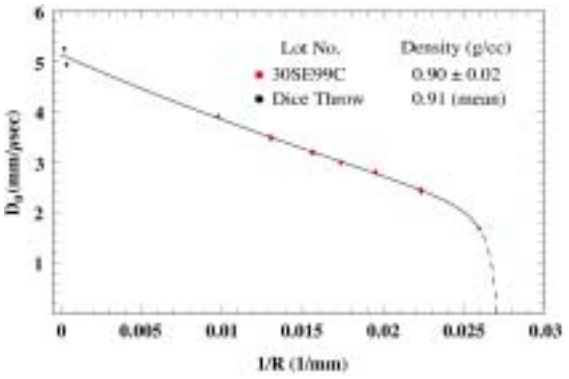

FIGURE 3. ANFO diameter effect data and curve fit.

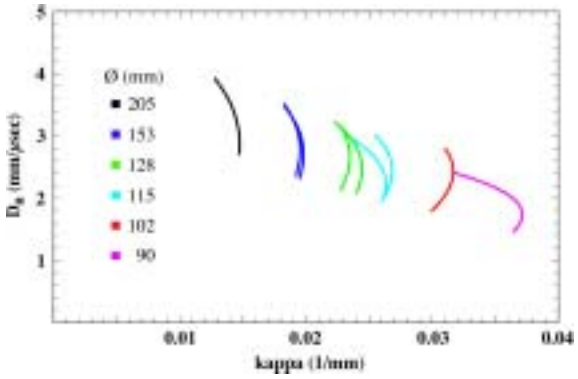

FIGURE 4. ANFO $D_n(\kappa)$ curves.

Diameter effect data, with Petes' included, and the fit to Eq. 5 are plotted in Fig. 3. Curve fit parameters are: D_∞ = 5.1464 mm/μsec, k_u = 0.09526 mm^{-1}, k_d = 0.02745 mm^{-1}, α = 1.6100 and β = 0.006523.

The $D_n(\kappa)$ curve is derived from D_0 and the slope $s(r)$ of the wave profile $z(r)$:

$$s(r) = \frac{dz(r)}{dr} = \tan\theta(r) \ , \qquad (6)$$

where $\theta(r)$ is the local angle between the charge axis and the normal direction to the wave front. The normal detonation velocity, D_n, is $D_0\cos\theta(r)$, or

$$D_n(r) = \frac{D_0}{\sqrt{1+s(r)^2}} \ . \qquad (7)$$

Total curvature, κ, is the sum of two terms:

$$\kappa(r) = \frac{s'(r)}{(1+s(r)^2)^{3/2}} + \frac{s(r)}{r\sqrt{1+s(r)^2}} \ . \qquad (8)$$

$D_n(\kappa)$ is generated by plotting $D_n(r)$ versus $\kappa(r)$. $D_n(\kappa)$ curves for the nine charges with front curvature records are shown in Fig. 4.

Unlike $D_n(\kappa)$ curves for PBX 9502[7] and nitromethane[8], ANFO $D_n(\kappa)$ curves 1) show little or no overlap, with smaller sticks lying to the right of larger ones, 2) exhibit a large velocity deficit with little κ variation, and 3) reach a maximum κ at an intermediate R. The $D_n(\kappa)$ curve for the 205 mm charge is nearly vertical, but the 90 mm curve is much flatter—perhaps because this charge is close to failure. Comparing the three sizes for which front curvatures are repeated, the 153 mm charges show excellent repeatability, while the 128 and 115 mm charges show the same general behavior, but differ from each other in detail. Nevertheless, the three listed characteristics seem to be real and consistent features of the data that deviate substantially from those of more ideal explosives, for which curves for different diameters overlay well for small κ but diverge for large κ, and for which κ increases mono- tonically with R. The behavior of Fig. 4 is com- patible neither with existing DSD implementation nor with current extensions[5]; however, it provides guidance for further extensions that consider the DSD consequences of disparate reaction rates[10].

ACKNOWLEDGEMENTS

We thank E. Aragon, R. Archuleta, M. Chavez, R. Critchfield, J. Keddy, D. Kennedy, and D. Murk for design/test support; R. Hopler and F. Sandstrom for data support; and R. Flesner for funding support.

REFERENCES

1. Yancik, J.J.; PhD Dissertation, Univ. of Missouri, 1960.
2. Petes, J., Miller, R., & McMullan, F.; DNA Technical Report No. DNA-TR-82-156, 1983.
3. Campbell, A.W., & Engelke, Ray; 6th International Detonation Symposium, 1976, pp. 642-652.
4. Wood, W.W., & Kirkwood, J.G.; J. Chem. Phys., 22, 1954, pp. 1920-1924.
5. Aslam, T.D.; Bdzil, J.B.; & Hill, L.G.; 11th International Detonation Symposium, 1998, pp. 21-29.
6. Sandstrom, F.W., Abernathy, R.L., Leone, M.G., & Banks, M.L.; 28th DOD Expl. Safety Board. Sem., 1998.
7. Hill, L.G., Bdzil, J.B., & Aslam, T.D.; 11th International Detonation Symposium, 1998, pp.1029-1037.
8. Hill, L.G., Bdzil, J.B., Davis, W.C., Engelke, R., & Frost, D.L.; Shock Compression of Condensed Matter, 1999, pp. 813-816.
9. Kennedy, D.L.; private communication, 2000.
10. Short, M., & Bdzil, J.B.; Submitted to J. Fluid Mech.